# Contents

# List of Tables



# List of Figures

# Chapter 1

# Introduction

Metamaterial has recently been extensively discussed and studied. This kind of artificial structure has been utilized for many guided and unguided wave applications. The unique characteristics have been considered to be valuable topics. Specifically left-handed materials (LHMs) possessing negative refractive index have drawn tremendous interests in both scientific and engineering fields. The new concept associated with LHMs has led to the development of materials and structures with unprecedented properties. In particular, it contributes to the antenna design for either the radiator itself [1–18]or the feeding structure [19–25]. The engineering application to small size antennas has surged in the last decades. Metamaterial antennas are expected to provide superior characteristics.

Several researches and applications [1–9] demonstrated practical approaches to synthesize LHMs based on the backward wave supported by a distributed or equivalent lumped ladder network. With the advantage of backfire-to-endfire scanning, electronically scanned leaky-wave antennas were designed for the desired operation characteristics.

The conventional right-handed transmission line (RH TL) theory illustrates the equivalent circuit model consisting of series per-unit-length in-

ductances and shunt per-unit-length capacitances. The analogy topology of series per-unit-length capacitances and shunt per-unit-length inductances indicates left-handed transmission lines (LH TL). Along the power travelling direction, LH TL is characterized by the advance phase changing whereas RH TL is characterized by the delay phase changing. RH TL and LH TL can be embedded into each other and was named as CRLH TL (Composite Right/Left- Handed Transmission Line) [26], which actually provides an idea to insert LH TL into the host RH TL. The zeroth-order resonance (ZOR) [27] makes use of the opposite phase properties of RH and LH TL and has been proved experimentally. Small planar antennas utilizing the ZOR structure were published [12–14]. The physical size of such antenna can be arbitrary regardless the operation frequency since it is specified by the value of the capacitances and inductances instead of the wavelength. The concept of the infinite wavelength resonant antenna was first demonstrated in [12]. However, it has relatively less compact size including the matching structure. Another published metamaterial antenna [13] consists of two substrate layers with one of which requiring quite small thickness and higher dielectric constant. The capability of dual-mode operation at two different frequencies was also presented in [14]. Other compact planar antennas using LH TL with periodically L-C loaded lines [10, 16] were presented. The investigated structures also demonstrated the possibility to reduce physical size of microstrip patch antennas. For all the recent published antennas above, patch or patch-like radiation patterns were obtained. There is, however, almost no focus topics on physical structure and radiation mechanism for the small antennas. This thesis intends to show the importance of the layout and the investigation for radiating.

Rather than employing CRLH or simply LH TL, a novel planar antenna utilizing cascaded right/left-handed transmission lines is proposed as

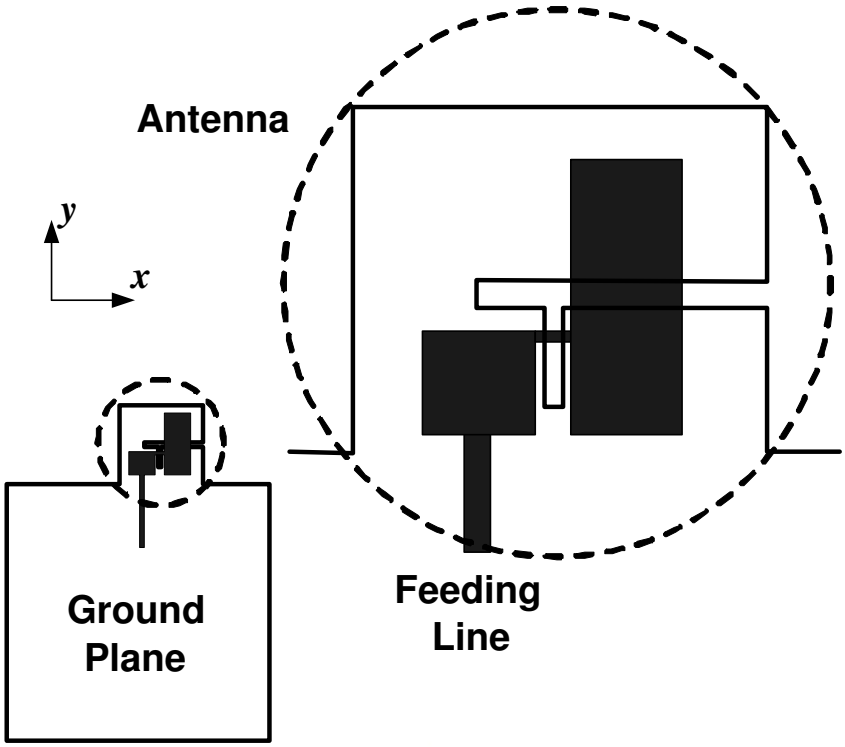


Figure 1.1: Geometry of the proposed planar antenna.

sketched in Fig. 1.1. Two cascaded transmission lines of equal amount of electrical length with opposite polarities, i.e. a segment of RH TL and a segment of LH TL, can also result in phase of zero degree. With using the equivalent transmission line circuits (EQC), one can realize compact antennas consisting of lumped inductances (L) and capacitances (C) on a printed circuit board without via. The physical dimension of the antenna is decided by the values of the inductances and capacitances. The layout planning has significant influences on the implementation of such radiating structures.

This thesis is organized as follows. Chapter 2 presents the equivalent transmission line model. Chapter 3 presents the design of the proposed antenna and compares different layouts. Chapter 4 discusses the radiation mechanism by investigating the simulation results. Two via-free printed antennas operating at GHz-range are demonstrated in Chapter 5. Finally, Chapter 6 concludes this study and draws some possible future works.

# Chapter 2

# Equivalent Transmission Line Model

Transmission line theory has long been a powerful analysis and design tool for conventional materials. The two-conductor transmission line system may be considered a distributed circuit and so is useful in establishing a relation between circuit theory and the more general electromagnetic theory expressed in Maxwell's equations.The concepts of energy propagation, reflections at discontinuities, standing versus travelling waves and the resonance properties of standing waves, phase and group velocity, and the effects of losses upon wave properties are easily extended from these transmission line results to the more general classes of guiding structures [28]. Conventionally the direction of the phase velocity is the same as that of the group velocity, which indicates the power travelling direction. It implies the tryad ($\overline{E}$, $\overline{H}$ ,$\overline{k}$) forms a right-handed system. However, recently LHM (Left-Handed Material) was proposed and verified for that the group velocity travels in the opposite direction against the phase velocity.

The design starts with cascading a segment of RH TL and a segment of LH TL. The former one has a positive electrical length indicating phase

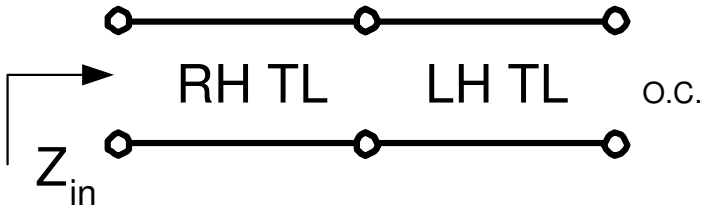


Figure 2.1: Cascaded right/left-handed transmission lines.

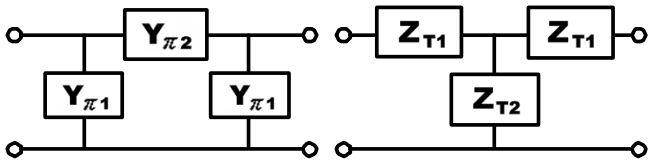


(a) (b)

Figure 2.2: The (a)$\pi$ (b)T equivalent circuit for a reciprocal two-port network.

delay whereas the latter one has a negative electrical length indicating phase advance. Having one port open-circuited as illustrated in Fig. 2.1, the input impedance possesses zero imaginary part, which is a basic requirement for resonance. By employing the equivalent circuit model for a TL segment, one can realize it with lumped circuits.

With the specified characteristic impedance $Z_0$, the operation frequency $f_0$, and the electrical length $\theta$, it is well-known that a certain length of transmission line can be modelled by either $\pi$ or T equivalent circuit. Fig. 2.2 shows the circuit models with

$$\begin{aligned} Y_{\pi 1} &= jY_0(\csc\theta - \cot\theta) \\ Y_{\pi 2} &= -jY_0 \csc\theta \\ Z_{T1} &= jZ_0(\csc\theta - \cot\theta) \\ Z_{T2} &= -jZ_0 \csc\theta \end{aligned} \tag{2.1}$$

where $Y_0 = 1/Z_0$. These formulas can be easily derived by comparing the

ABCD matrix for TL segment with the ABCD matrix for $\pi$ and T circuits at the design frequency [29]. The trigonometric functions for the normalized component values with $Y_0 = 1$ and $Z_0 = 1$ are sketched in Fig. 2.3. The upper half plane in Fig. 2.3(a) and the lower plane in Fig. 2.3(b) indicate capacitive elements whereas the lower half plane in Fig. 2.3(a) and the upper plane in Fig. 2.3(b) indicate inductive elements.

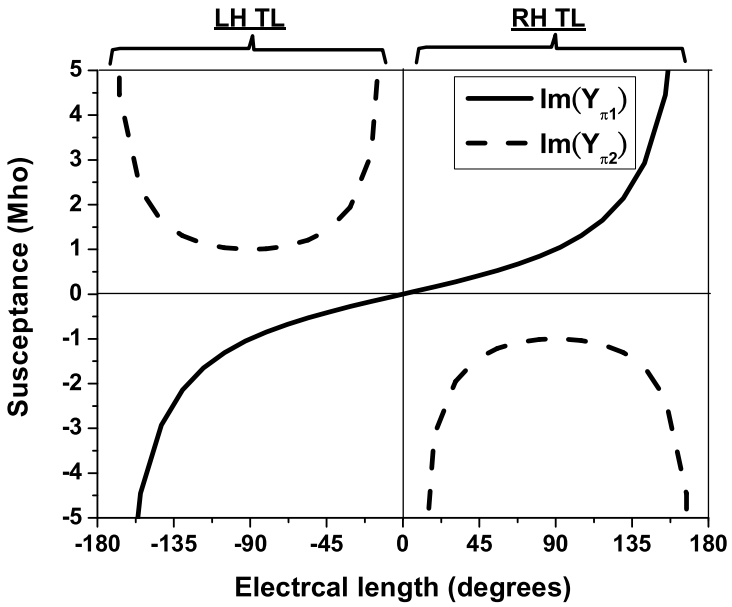


(a)

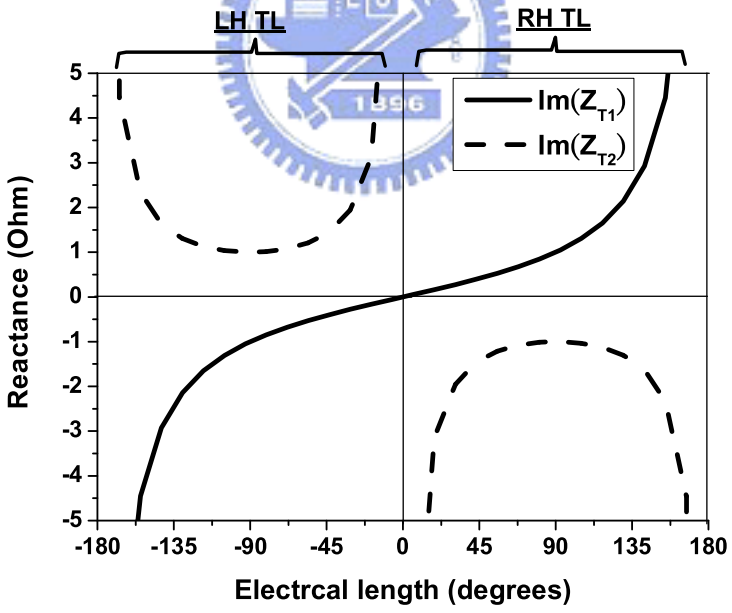


(b)

Figure 2.3: The (a)susceptance (b)reactance of the EQC elements versus the electrical length.

# Chapter 3

# Design and Layout

## 3.1 Design of Circuit Parameters

Following the previous section, formulas for the inductors (L) and capacitors (C) of equivalent transmission line model are listed in Table 3.1, where $\omega_0 = 2\pi f_0$. The notation $L_{L\pi}$, for example, represents the value of the inductor of the $\pi$ model for LH TL. Since each segment in Fig. 2.1 can employee either $\pi$ or T circuit, there are four combinations in total. A $\pi$ circuit for RH TL and a T circuit for LH TL are chosen and connected with an open-circuit at the unconnected port of the LH TL. This can results in a via-free layout which does not require an extra fabrication process and higher cost. The capacitor connected to the open-circuit end is removed due to circuit analysis, which also reduces the number of the elements. As shown in Fig. 3.1, it turns out the circuit for designing the proposed antenna where $C_1 = C_2 = C_{R\pi}$, $L_1 = L_{R\pi}$, $C_3 = C_{LT}$, and $L_2 = L_{LT}$.

In order to have a compact structure, the design of the circuit parameters was considered. Referring to Fig. 2.3, choosing $\theta$ close to either 0 or 180 degrees leads to very large L or C value. Therefore, $\theta$ is chosen to be 90 degrees. In addition, since many published antennas using metamater-

Table 3.1: Formulas of L and C for a TL segment

| EQC | Formulas for L | Formulas for C |
|---|---|---|
| $\pi_{LH}$ | $L_{L\pi}=\frac{Z_0}{(\csc\theta-\cot\theta)\omega_0}$ | $C_{L\pi}=\frac{1}{Z_0\omega_0\sin\theta}$ |
| $\pi_{RH}$ | $L_{R\pi}=\frac{Z_0\sin\theta}{\omega_0}$ | $C_{R\pi}=\frac{(\csc\theta-\cot\theta)}{Z_0\omega_0}$ |
| $T_{LH}$ | $L_{LT}=\frac{Z_0}{\omega_0\sin\theta}$ | $C_{LT}=\frac{1}{Z_0\omega_0(\csc\theta-\cot\theta)}$ |
| $T_{RH}$ | $L_{RT}=\frac{Z_0(\csc\theta-\cot\theta)}{\omega_0}$ | $C_{RT}=\frac{\sin\theta}{Z_0\omega_0}$ |

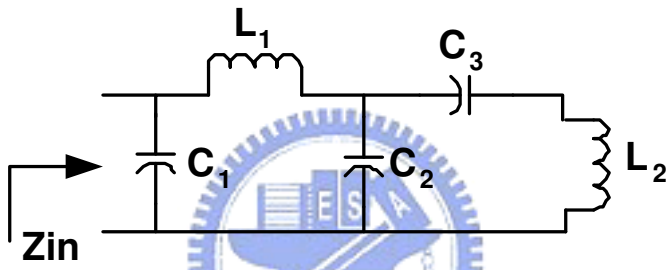


Figure 3.1: Cascaded circuit structure consisting of a $\pi$ model for RH TL and a T model for LH TL.

ial concepts, mentioned in Section 1, possess patch or patch-like radiation patterns, this study goes with introducing relatively larger capacitors rather than larger inductors. In case of avoiding large inductors and mainly having patches in the physical structure, a relatively small characteristic impedance is preferred.

## 3.2 Layout

For planning the layouts, full wave EM simulation is done by utilizing the commercial software, Ansoft HFSS. The operation frequency is 2.45 GHz and

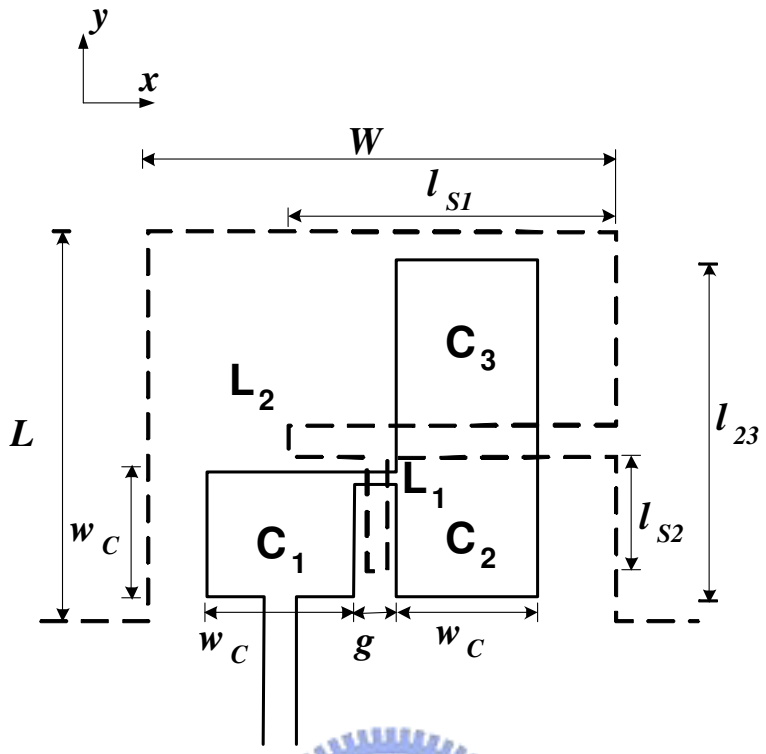


Figure 3.2: Layout of the proposed antenna. The dashed lines are for the bottom metal layout and the solid lines are for the top metal layout. (Top view)

the characteristic impedance ($Z_0$) is set to be 25 Ohm. It turns out all the three capacitors have the same value of 2.6 pF and both the two inductors have the same value of 1.26 nH at the operation frequency. Three possible layouts are considered as follows.

A compact antenna structure based on the circuit in Fig. 3.1 is proposed as illustrated in Fig. 3.2 with the corresponding elements marked. The rectangular patches are obviously planned to realize metal insulator metal (MIM) capacitors. The narrow short metal traces dominantly contribute as inductors. The geometry parameters are $L = W = 11.5\ mm$, $w_C = 4\ mm$, $L_23 = 9.5\ mm$, $g = 1.3\ mm$, $L_{S1} = 9\ mm$, $L_{S2} = 3.2\ mm$. Instead of a narrow short trace, this small inductor $L_2$ is realized by a wide and longer

metal trace. Besides, a slot under $L_1$ is introduced and observed to provide a wide tuning range for the input resistance by changing the slot length, $l_{S2}$.

Two other possible layouts, named the type A and B, are shown in Fig. 3.3(a) and Fig. 3.3(b) also with the corresponding elements marked. For the type A layout, the bottom pattern is a wide trace of 5.5 mm in width with, of course, a narrow trace for $L_2$. The top pattern is a less wide trace of 3.5 mm in width also with a narrow trace of 2.5 mm in length for $L_1$ as it is in the proposed layout. The type B layout has quite similar dimension with the A layout but its wide traces going along a edge of the ground plane. The trace for $L_2$ is then less narrow. The dimension along the y axis of the straight type A antenna is 18.5 mm and the dimension along the x axis of the straight type B antenna is 18 mm. It can be roughly interpreted that the proposed layout is obtained by bending the more straight layout as the type A or B. The simulated input impedances of both antennas possess zero imaginary part and relatively large real part shown in Fig. 3.4. It should be mentioned that all the three layouts have finite ground planes of 40 mm by 30 mm in size, extended in the negative y direction and partly ignored for simplicity of illustration.

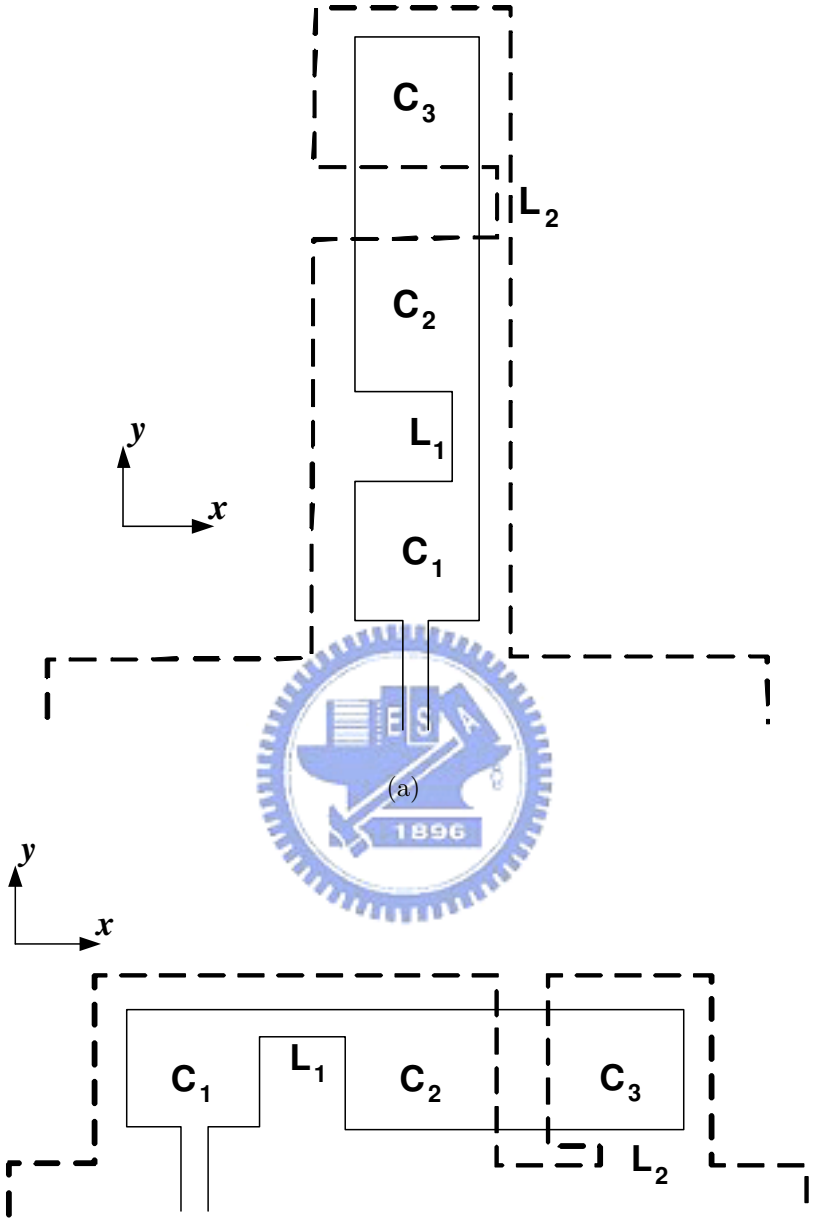


(b)

Figure 3.3: Layout of the (a) type A (b) type B antenna. The dashed lines are for the bottom metal layout and the solid lines are for the top metal layout. (Top view)

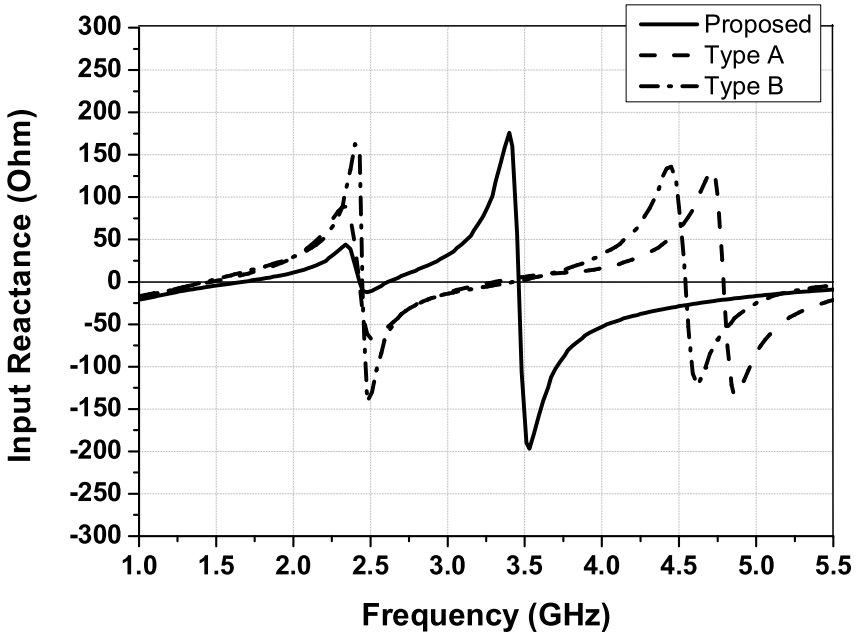


(a)

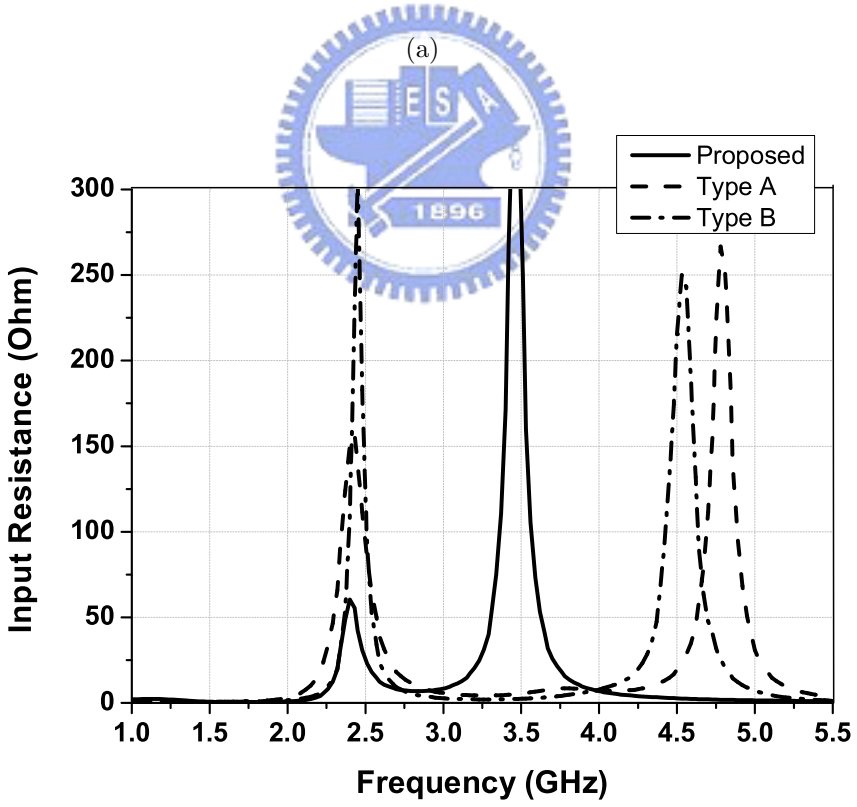


(b)

Figure 3.4: Simulated input (a) reactance and (b) resistance for all the three different layouts.

# Chapter 4

# Radiation Mechanism

## 4.1 Radiation Mechanism

As the simulation results in the previous chapter, the layout planning has significant influences on providing efficient radiating structures while employing the cascaded right/left-handed transmission lines. Different layouts cause different electric field and current distribution which dominate the radiation mechanism. An individual patch of small size with respect to the wavelength can not generate far field radiation since the equivalent surface magnetic current ($\mathbf{M_S}$) at the edges results in cancelling each other. A surface magnetic current $\mathbf{M_S}$ is defined by

$$\mathbf{M_S} = \mathbf{E} \times \widehat{\mathbf{n}} \tag{4.1}$$

where $\mathbf{E}$ is the electric field and $\widehat{\mathbf{n}}$ is the normal vector to the surface. However, though carefully design and layout planning, the proposed antenna physically formed by small patches and slots can offer fairly good performance with the compact dimension of $\lambda_0/12$ square, where $\lambda_0$ is the free space wavelength.

The proposed layout has a topology of patches at the top and slots at the

bottom. The bottom pattern could be considered as the extended ground with two connected orthogonal slots. Both the circuit analysis and the full wave simulation indicate a virtual ac ground at the interconnection between $C_2$ and $C_3$ for the operation frequency. The MIM capacitors confine electric energy and provide fringing fields at their edges. As seen in Fig. 4.1(a), the electric field for $C_2$ and $C_3$ possesses opposite polarities, i.e. the electric field vectors for $C_2$ points upward if those for $C_3$ points downward. The opposite polarities make the equivalent magnetic current flow from $C_2$ goes clockwise while that from $C_3$ goes counterclockwise. Fig. 4.1(b) shows the equivalent magnetic current distribution. The close and opposite directed pairs of the magnetic currents cancel each other. Therefore, as a result, there are two edges at the top constructively contributing to radiation. These two edges provided by $C_2$ and $C_3$ at the top side operate as the radiating edges of a conventional half-wavelength patch antenna. In other word, this design shrinks the dimension from half wavelength to one-twelfth wavelength. Moreover, there are two connected slots at the bottom side offer aperture electric field to radiate. This topology results in more radiating structures. The contribution provided by $C_1$ is not taken into account since its field strength is very weak.

Regarding the type A, it plans three patches in a row with two short traces. As seen in Fig. 4.2(b), the equivalent magnetic current distribution is indicated by the two-headed arrows. The ones provided by $C_1$ cancel each other in the far field since they are close and opposite directed in pairs. The fringing field from $C_2$ is too weak to contribute. Two remaining edges provide equivalent magnetic currents in the same direction. One is from the slot at the bottom side between $C_2$ and $C_3$. The other one from one of the edges of $C_3$ is close and parallel to the previous one. The type B has very similar field distribution with the type A.

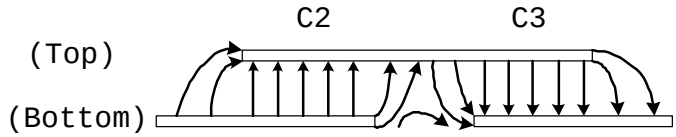


(a)

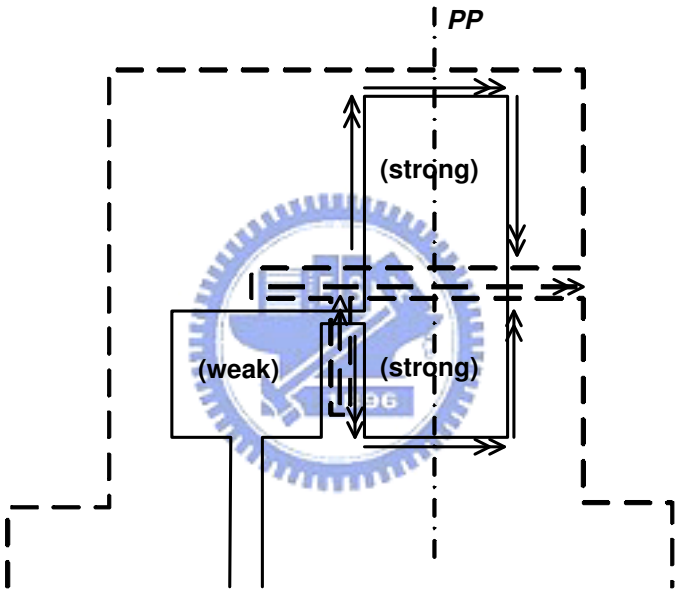


(b)

Figure 4.1: (a)Schema of the electric field distribution at the PP cut for the proposed antenna.(Side view) (b)Schema of the equivalent magnetic current distribution for the proposed antenna.(Top view)

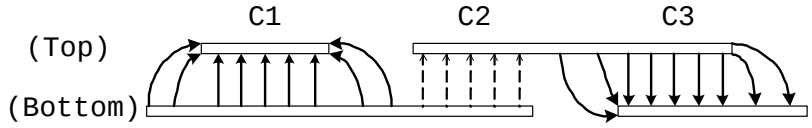


(a)

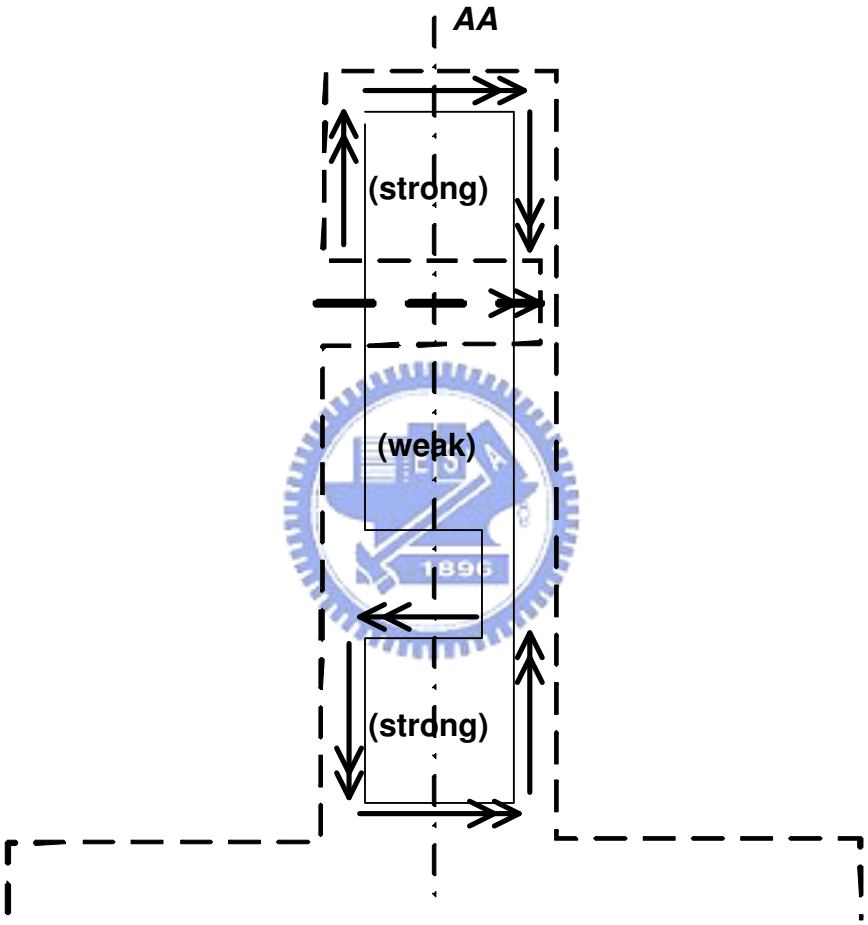


(b)

Figure 4.2: (a)Schema of the electric field distribution at the AA cut for the type A antenna.(Side view) (b)Schema of the equivalent magnetic current distribution for the type A antenna.(Top view)

## 4.2 Patches and Slots of the Proposed Antenna

The proposed antenna structure can be interpreted as closing the layout for $L_2$ to the bottom side of $C_1$. The surface electric current flow is guided roughly in a loop in the order of $C_1$, $L_1$, $C_2$, $C_3$, $L_2$ and then back to $C_1$. It results in the cancellation of the opposite current flows at $C_1$, which makes the field intensity weak at $C_1$ and strong at $C_2$. Thereby, two patches for $C_2$ and $C_3$ with intense field forms four constructively radiating edges, two at the top and two at the bottom. Different from the proposed structure, the layout for $L_2$ in the type A directly connects to the nearest element $C_3$, which causes weak field intensity at $C_2$. The consequence of the intense field at $C_1$ as an individual small patch does not radiate. As a result, the layout of the proposed antenna offers more radiating edges. It is considered as a more efficient layout with respect to radiating structures.

The aperture electric field contributes to radiating from the connected slots at the bottom side. In addition to the consideration of the surface electric current flow discussed above, another reason to bend the layout is the result of investigating the simulated electric field distribution, i.e. the patches for the segment of RH TL, $C_1$ and $C_2$, and the one for the segment of LH TL, $C_3$, introduce oppositely polarized electric field. Therefore, aperture electric field tangential to the x-y plane is expected and actually observed by planning these two TL segments parallel to each other. Furthermore, the slot under $L_1$ is introduced to avoid the image electric current of $L_1$ for shorten the trace length of $L_1$. It is found that the slot length, $l_{S2}$, can be used to reduce the input resistance of the antenna from hundreds of ohms to a few ohms shown in Fig. 4.3. The slot has to be connected to the longer slot between $C_2$ and $C_3$ to have the desired behavior. The aperture electric field

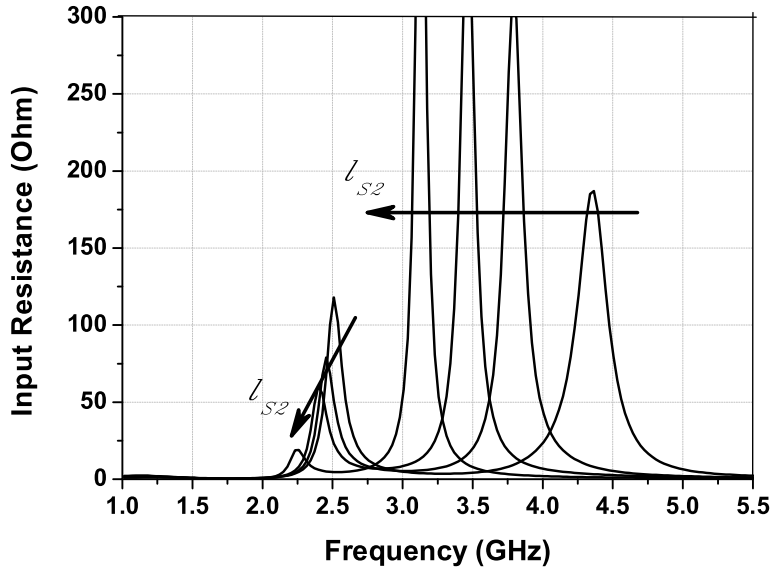


(a)

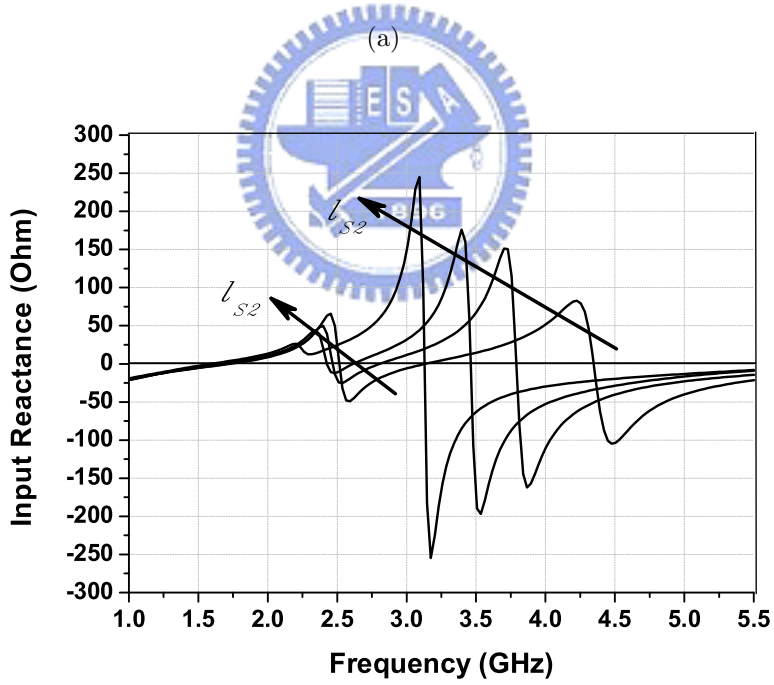


(b)

Figure 4.3: Simulated (a)real (b)imaginary part of the input impedance with changing the slot length under $L_1$.

from this shorter slot does not destruct other radiating contribution since it is orthogonal to the others.

# Chapter 5

# Measurements

For experimental verification, both the type A and the proposed structure are fabricated and measured. These two printed antennas were implemented on an FR4 substrate with relative dielectric constant of 4.4 and thickness of 0.4 mm. The proposed antenna results in occupying an area of 11.5 mm square and its ground size is of 40 mm by 35 mm. The type A has the size of 5.5 mm by 18.5 mm with the the same ground size as the proposed one. They both are feeded at the end of the microstrip line by 50-Ω coaxial cable from the back side. As the simulation result expected, the input resistance of the type A antenna is relatively large for the 50-Ω system. Thus, an extra 18-mm high impedance line is added between C1 and the 50-Ω microstrip feeding line.

By measurements, due to fabrication techniques, both of the antennas have frequency shift from the desired 2.45GHz to 2.23 GHz for the proposed antenna and to 2.35GHz for the type A antenna with the measured return loss of 23 and 16 dB, respectively, shown in Fig. 5.1. The 10-dB return loss bandwidth is 4.48% and 5.32%, respectively, for the proposed and type A antennas. Fig. 5.2 and Fig. 5.4 show the photographs of the antennas. Both the fabricated antennas have fairly omnidirectional far field radiation

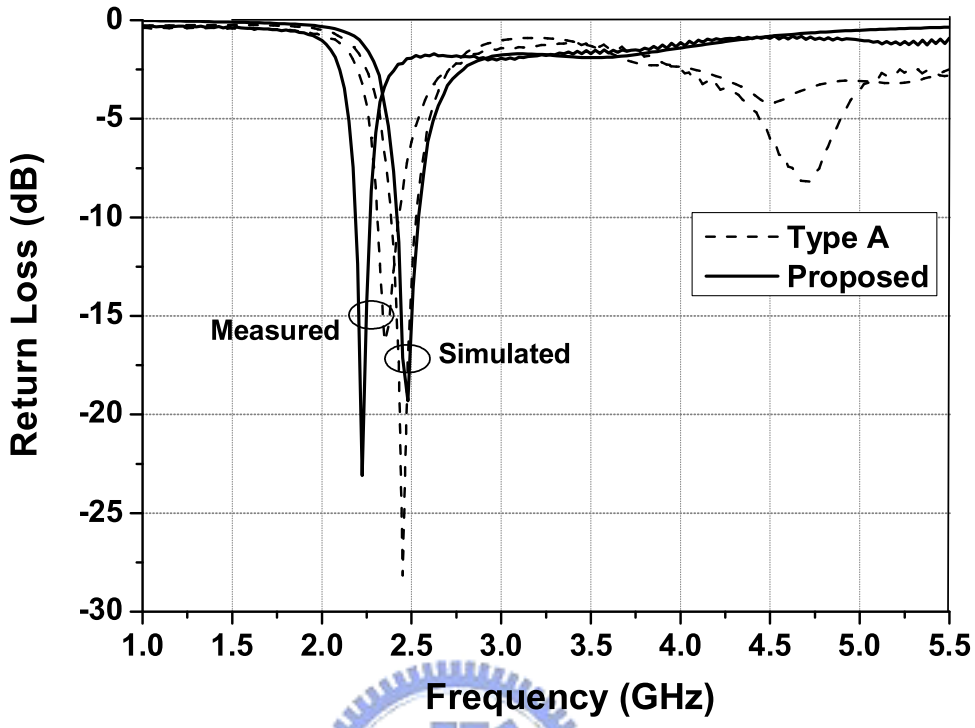


Figure 5.1: Simulated and measured return loss for the proposed and type A antennas.

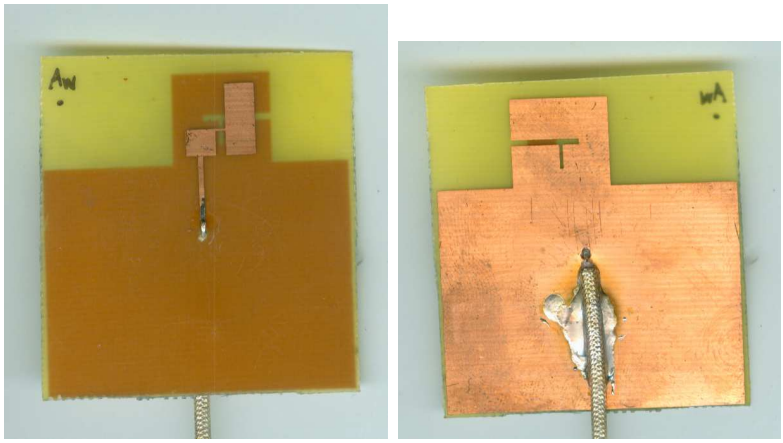

(a) (b)

Figure 5.2: Photographs of the proposed antenna in the (a) top and (b) bottom view.

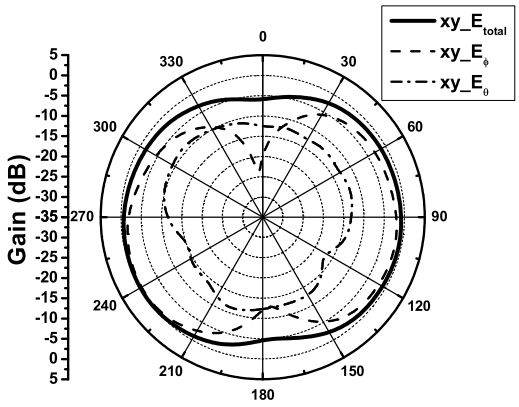


(a)

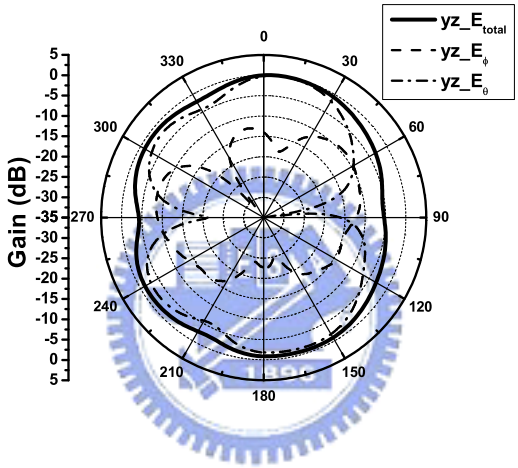


(b)

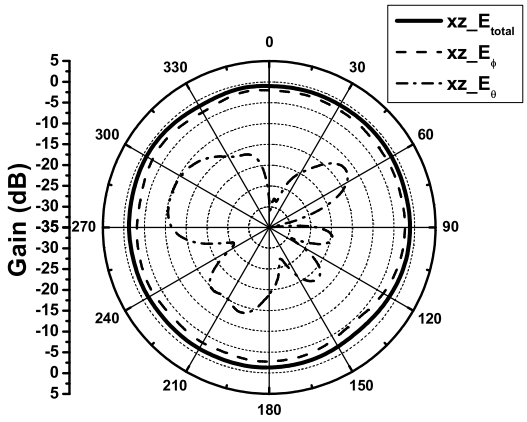


(c)

Figure 5.3: Measured radiation patterns for the proposed antenna in (a) x-y, (b) y-z, and (c) x-z planes, respectively

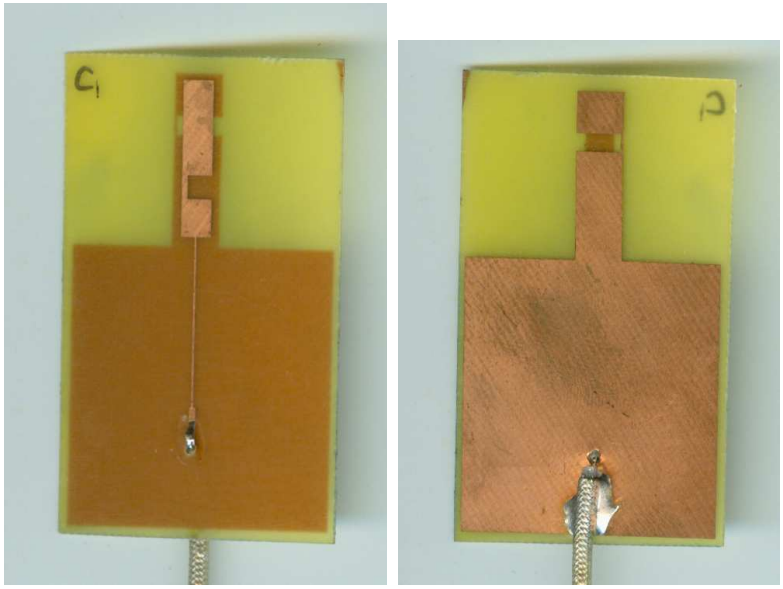

(a) (b)

Figure 5.4: Photographs of the type A antenna in the (a) top and (b) bottom view.

patterns in three principal planes. Fig. 5.3 shows the measured radiation patterns for the proposed antenna in x-y, y-z, and x-z planes with average gain of -2.04, -1.41, -1.02 dB, respectively. Fig. 5.5 shows the measured radiation patterns for the type A antenna in x-y, y-z, and x-z planes with average gain of -2.01, -1.72 and -1.80 dB, respectively. The maximum gain is +0.16 and -0.54 dB for the proposed and type A antennas, respectively.

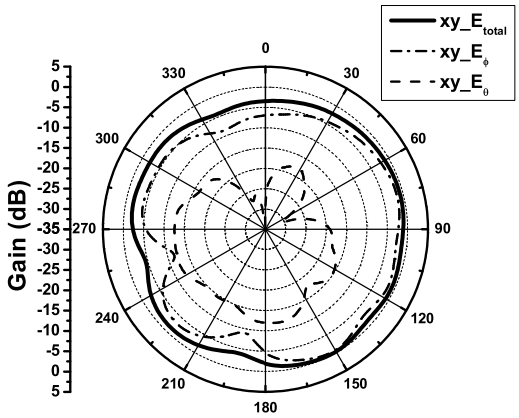


(a)

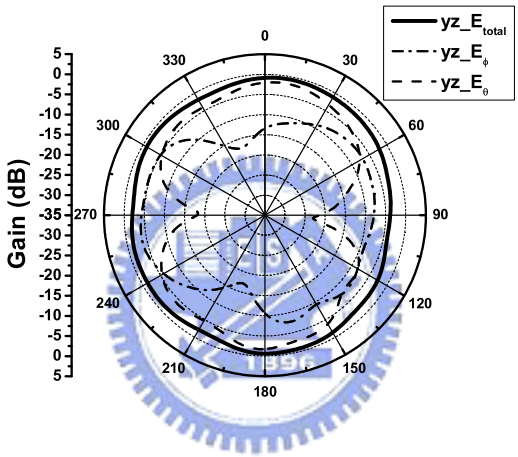


(b)

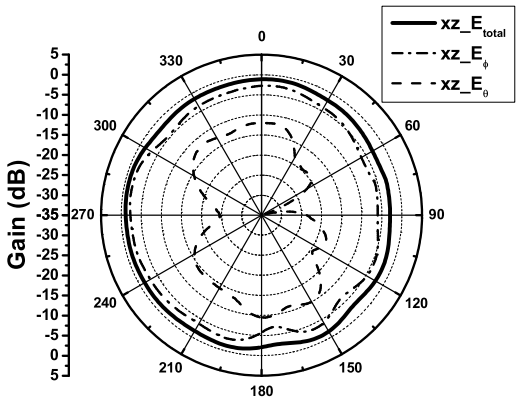


(c)

Figure 5.5: Measured radiation patterns for the type A antenna in (a) x-y, (b) y-z, and (c) x-z planes, respectively

# Chapter 6

# Conclusion

A novel compact planar antenna is designed and verified experimentally. Fairly good measurement results are obtained. Layout planning plays a crucial role for radiating as discussed. Different layouts for the same circuit model can cause different performances. This thesis shows the possibility to design compact antennas based on cascaded right/left-handed transmission lines. Though applying the equivalent transmission line model, the physical dimension can be compact ($\lambda_0/12$) with providing more radiating edges. The proposed cascaded right/left-handed transmission lines can be utilized for antenna design. Based on the high-pass topology for LH TL, many published realizations on printed circuit board, mentioned in 1, have developed edge or broadside coupling for capacitance and via holes for inductance. For some of them, the host medium were analytically taken into consideration. Usually more than one unit-cell were introduced repeatedly. In this thesis, the proposed antenna avoids via and consists of five lumped elements by the selection of the EQC model combination. The $\pi$ and T models can offer exact formulas for L and C for almost all-range electrical length, $\theta$, rather than CRLH TL of which formulas for the circuit elements are valid for very small $\theta$ with the same accuracy as $\sin\theta$ approaches 1. Instead of only half-

space patch-alike radiation, the proposed antenna structure with more than two radiating edges gives all the three principal planes fairly omnidirectional radiation patterns. Additionally, although the equivalent circuit parameters in this paper are chosen for certain considerations, different electrical length, different characteristic impedance, or different equivalent models are still possible to be applied for different purposes. However, the radiation mechanism may also be different since layout is crucial.

# Bibliography


[1] L. Liu, C. Caloz, and T. Itoh, "Dominant mode leaky-wave antenna with backfire-to-endfire scanning capability," *Electronics Letters,* Vol.38, pp.1414-1416, Nov. 2002.

[2] S. Lim, C. Caloz, and T. Itoh, "A reflectodirective system using a composite right/left-handed (CRLH) leaky-wave antenna and heterodyne mixing," *IEEE Microwave and Wireless Comp. Lett.,* Vol.14, pp.183-185, Apr. 2004.

[3] C. A. Allen, C. Caloz, and T. Itoh, "Leaky-waves in a metamaterial-based two-dimensional structure for a conical beam antenna application," *IEEE MTT-S Int. Microwave Symp. Dig.,* Vol.1, pp.305-308, Jun. 2004.

[4] C. Caloz and T. Itoh, "Array factor approach of leaky-wave antennas and application to 1-D/2-D composite right/left-handed (CRLH) structures," *IEEE Microwave and Wireless Components Lett.,* Vol.14, pp.274-276, Jun. 2004.

[5] S. Lim, C. Caloz, and T. Itoh, "Electronically scanned composite right/left handed microstrip leaky-wave antenna," *IEEE Microwave and Wireless Components Lett.,* Vol.14, pp.277-279, Jun. 2004.

[6] S. Lim, C. Caloz, and T. Itoh, "Metamaterial-based electronically controlled transmission-line structure as a novel leaky-wave antenna with tunable radiation angle and beamwidth," *IEEE Trans. Microwave Theory and Techniques,* Vol.53, pp.161-173, Jan. 2005.

[7] S. Matsuzawa, K. Sato, A. Sanada, H. Kubo, and S. Aso, "Left-handed leaky wave antenna for millimeter-wave applications," *IEEE Int. Workshop on Antenna Technology Small Antennas and Novel Metamaterials,* pp.183-186, Mar. 2005.

[8] C. A. Allen, K. M. K. H. Leong, C. Caloz, and T. Itoh, "A two-dimensional edge excited metamaterial-based leaky wave antenna," in *Proc. IEEE Antennas Propag. Soc. Int. Symp.,* Vol.2B, pp.320-323, Jul. 2005.

[9] K. Sato, S. Matsuzawa, Y. Inoue, and T. Nomura, "Electronically scanned left-handed leaky wave antenna for millimeter-wave automotive applications," *IEEE Int. Workshop on Antenna Technology Small Antennas and Novel Metamaterials,* pp.420-423, Mar. 2006.

[10] M. Schussler, J. Freese, and R. Jakoby, "Design of compact planar antennas using LH-transmission lines," *IEEE MTT-S Int. Microwave Symp. Dig.,* Vol. 1, 6-11, Jun. 2004.

[11] A. Sanada, K. Murakami, S. Aso, H. Kubo, and I. Awai, "A via-free microstrip left-handed transmission line," *IEEE MTT-S Int. Microwave Symp. Dig.,* Vol.1, pp. 301-304, Jun. 2004.

[12] A. Sanada, M. Kimura, I. Awai, C. Caloz, and T. Itoh, "A Planar zeroth-order resonator antenna using a left-handed transmission line," *European Microwave Conference*, Amsterdam, Netherlands, pp. 1341-1344, Oct. 2004.

[13] C.-J. Lee, K. M. K. H. Leong, and T. Itoh, "Design of resonant small antenna using composite right/left-handed transmission line," *IEEE Antenna Propag. Soc. Int. Symp.*, Vol. 2B, pp. 218-221, Jul. 2005.

[14] A. Lai, K. M. K. H. Leong, and T. Itoh, "Dual-mode compact microstrip antenna based on fundamental backward wave," in *Proc. Asia-Pacific Microwave Conf.,* Vol.4, Suzhou, China, Dec. 2005.

[15] S. Otto, A. Rennings, C. Caloz, P. Waldow, and T. Itoh, "Composite right/left-handed $\lambda$-resonator ring antenna for dual-frequency operation," in *Proc. IEEE Antennas Propag. Soc. Int. Symp.,* Vol.1A, pp.684-687, Jul. 2005.

[16] M. Schussler, C. Damm, J. Freese, and R. Jakoby, "Realization concepts for compact microstrip antennas with periodically loaded lines," *IEEE MTT-S Int. Microwave Symp. Dig.,* 12-17, Jun. 2005.

[17] Z. Qi and L. Huan, "Design of printed antenna with left-handed array," in *Proc. Asia-Pacific Microwave Conf.,* Vol.4, Suzhou, China, Dec. 2005.

[18] A. Lai, K. M. K. H. Leong, and T. Itoh, "Composite right/left-handed metamaterial antennas," *IEEE Int. Workshop on Antenna Technology Small Antennas and Novel Metamaterials,* Mar. 6-8, 2006, pp. 404-407.

[19] C.-J. Lee, K. M. K. H. Leong, and T. Itoh, "A broadband microstrip-to-CPS transition using composite right/left-handed transmission lines with an antenna application," *IEEE MTT-S Int. Microwave Symp. Dig.,* 12-17, Jun. 2005.?????

[20] K. Z. Rajab, R. Mittra, and M. T. Lanagan, "Size reduction of microstrip antennas using metamaterials," in *Proc. IEEE Antennas Propag. Soc. Int. Symp.,* Vol.2B, pp.296-299, Jul. 2005.

[21] A. Lai, K. M. K. H. Leong, and T. Itoh, "Novel series divider for antenna arrays with arbitrary element spacing based on a composite right/left-handed transmission line," *2005 European Microwave Conference,* Vol.1, pp.145-148, Oct. 2005.

[22] Z. Zhang and S. Xu, "A novel feeding network with composite right/left-handed transmission line for 2-dimension millimeter wave patch arrays," in *Proc. Asia-Pacific Microwave Conf.,* Vol.3, Suzhou, China, Dec. 2005.

[23] S.-G. Mao and Y.-Z. Chueh, "Broadband composite right/left-handed coplanar waveguide power splitters with arbitrary phase responses and balun and antenna applications," *IEEE Trans. Antennas and Propagation,* Vol.54, pp.234-250, Jan. 2006.

[24] H. Iizuka and P. S. Hall, "A left-handed dipole concept," *IEEE Int. Workshop on Antenna Technology Small Antennas and Novel Metamaterials,* pp.396-399, Mar. 2006.

[25] S.-G. Mao and S.-L. Chen, "Characterization and modeling of left-handed microstrip lines with application to loop antennas," *IEEE Trans. Antennas and Propagation,* Vol.54, pp.1084-1091, Apr. 2006.

[26] C. Caloz and T. Itoh, "Novel microwave devices and structures based on the transmission line approach of meta-materials," *IEEE MTT-S Int. Microwave Symp. Dig.,*, Jun. 2003, pp. 195-198.

[27] A. Sanada, C. Caloz, and T. Itoh, "Novel zeroth-order resonance in composite right/left-handed transmission line resonators," in *Proc. Asia-Pacific Microwave Conf.*, pp. 1588-1592, Seoul, Korea, Nov. 2003.

[28] S. Ramo, J. R. Whinnery, and T. Van Duzer, "Fields and Waves in Communication Electronics," Chapter 5, 3rd ed. New York:Wiley,1994.

[29] D. Kuylenstierna, S. E. Gunnarsson and H. Zirath, "Lumped-element quadrature power splitters using mixed right/left-handed transmission lines," *IEEE Trans. Microwave Theory and Techniques,* Vol.53, pp.2616-2621, Aug. 2005.